Available online at www.sciencedirect.com
SCIENCE DIRECT®
Journal of Solid State Chemistry 178 (2005) 3554–3562
JOURNAL OF SOLID STATE CHEMISTRY
www.elsevier.com/locate/jssc

Two new two-dimensional organically templated phosphite compounds: $(C_6H_{16}N_2)_{0.5}[M(HPO_3)F]$, M = Fe(II) and Co(II): Solvothermal synthesis, crystal structures, thermal, spectroscopic, and magnetic properties

Sergio Fernández-Armas[a], José L. Mesa[a,*], José L. Pizarro[b], U-Chan Chung[b], María I. Arriortua[b], Teófilo Rojo[a,*]

[a]Departamento de Química Inorgánica, Facultad de Ciencia y Tecnología, Universidad del País Vasco, Apdo. 644, E-48080 Bilbao, Spain
[b]Departamento de Mineralogía y Petrología, Facultad de Ciencia y Tecnología, Universidad del País Vasco, Apdo. 644, E-48080 Bilbao, Spain

Received 27 May 2005; received in revised form 7 September 2005; accepted 11 September 2005
Available online 19 October 2005

Abstract

The organically templated $(C_6H_{16}N_2)_{0.5}[M(HPO_3)F]$ [M(II) = Fe (**1**) and Co (**2**)] compounds have been synthesized by using mild hydrothermal conditions under autogeneous pressure. The crystal structures have been determined from X-ray single-crystal diffraction data. The compounds are isostructural and crystallize in the $C2/c$ monoclinic space group. The unit-cell parameters are $a = 5.607(1)$, $b = 21.276(4)$, $c = 11.652(1)$ Å, $\beta = 93.74(1)^\circ$ for the iron phase and $a = 5.5822(7)$, $b = 21.325(3)$, $c = 11.4910(1)$ Å, $\beta = 93.464(9)^\circ$ for the cobalt compound with $Z = 4$. The crystal structure of these compounds consists of $[M(HPO_3)F]^-$ anionic sheets. The layers are constructed from chains which contain $[M_2O_6F_3]$ dimeric units linked by fluoride ions. The *trans*-1,4-diaminocyclohexane cations are placed in the interlayer space. The IR and Raman spectra show the bands corresponding to the phosphite oxoanion and organic dication. The Dq and Racah (B and C) parameters have been calculated from the diffuse reflectance spectra in the visible region. Dq parameter is 790 cm^{-1} for compound (**1**). For phase (**2**) the Dq value is 725 cm^{-1} and B and C are 930 and 4100 cm^{-1}, respectively. The thermal evolution of the molar magnetic susceptibilities of these compounds show maxima at 20.0 and 6.0 K for the iron(II) and cobalt(II) phases, respectively. These results indicate the existence of antiferromagnetic interactions in both compounds.

Keywords: Solvothermal synthesis; Thermal behavior; X-ray diffraction; IR; UV/Vis; Magnetic behavior.

1. Introduction

The synthesis of novel, open-framework, organically templated metal compounds under hydrothermal conditions represents a major activity in current solid-state chemistry. They are of scientific interest because of the challenges posed by their synthesis, processing and characterization. Many of these materials are synthesized in the presence of organic amines as structure-directing agents, usually accommodated in the structural voids and not as a part of the inorganic skeleton. The extended inorganic networks templated by organic cations now cover a remarkable range of compositions and structures [1]. With inspiration from the examples of aluminosilicate zeolites, the applications of some of these materials as catalysts [2], absorption agents [3] and ion exchangers [4] have been investigated. Two areas of particular interest to synthetic and structural chemists are to devise rational and reliable syntheses for these materials [5] and to understand the resulting, often complicated, crystal structures.

In recent years, considerable effort has been devoted to designing open-framework inorganic materials other than phosphates, such as chalcogenides, pnictides, cyanides, and thiopnictides [6,7]. Although the majority of the inorganic

*Corresponding authors. Fax: +34 946013500.
E-mail addresses: qipmeruj@lg.ehu.es (J.L. Mesa), qiproapt@lg.ehu.es (T. Rojo).

0022-4596/$ - see front matter © 2005 Elsevier Inc. All rights reserved.
doi:10.1016/j.jssc.2005.09.032

open-framework structures reported in the literature are silicates [8], phosphates [1], or carboxilates [9], there have been recent reports of open-framework structures synthetized using other anion units. The possibilities of incorporating phosphorous(III) as pseudo-pyramidal $(HPO_3)^{2-}$ hydrogen phosphite into extended structures templated by inorganic alkaline earth cations were explored [10]. However, the inorganic–organic hybrid phosphites with metallic transition elements have not been extensively studied, and only compounds with V(IV), Co(II), Mn(II), Fe(II, III), V(III), Cr(III) cations are known [11]. In order to complete the knowledge about this type of microporous materials incorporating metallic magnetic cations belonging to the first series of transition elements we have synthesized the phosphites $(C_6H_{16}N_2)_{0.5}[M(HPO_3)F]$, where M is Fe(II) and Co(II). In the present work, we report the solvothermal synthesis, crystal structures, thermal, and the spectroscopic and magnetic properties.

2. Experimental section

2.1. Synthesis and characterization

$(C_6H_{16}N_2)_{0.5}[M(HPO_3)F]$ [M = Fe (**1**) and Co (**2**)] were prepared under mild hydrothermal conditions under autogeneous pressure. Stoichiometric quantities of $FeC_2O_{4.2}H_2O$ (0.73 mmol) or $CoCl_2 \cdot 6H_2O$ (3.0 mmol), for phases (**1**) and (**2**), respectively, H_3PO_3 (7.5 mmol), HF (1 or 1.5 mL) and *trans*-1,4-diaminocyclohexane up to a pH between 4 and 6, were dissolved in 4:1 water:ethanol (25 mL) and stirred up to homogeneity. They were then placed in PTFE-lined stainless steel pressure vessels (fill factor 75%) and heated at 170 °C for 5 days, followed by slow cooling to room temperature. The pH of the mixtures did not show any appreciable change during the hydrothermal reactions. The compounds were obtained in the form of single-crystals, colorless for (**1**) and of red color for (**2**). The percentage of the elements in the products was calculated by inductively coupled plasma atomic emission spectroscopy (ICP-AES) and C, H, N-elemental analysis. Fluoride content was determined using a selective electrode. Found: Fe, 25.8; P, 14.2; C, 16.5; H, 4.0; N, 6.3; F, 8.6. $(C_6H_{16}N_2)_{0.5}$ [Fe(HPO_3)F] requires Fe, 26.2; P, 14.5; C, 16.9; H, 4.3; N, 6.6; F, 8.9. Found: Co, 27.0; P, 14.1; C, 16.1; H, 3.9; N, 6.3; F, 8.7. $(C_6H_{16}N_2)_{0.5}$[Co(HPO_3)F] requires Co, 27.3; P, 14.3; C, 16.7; H, 4.2; N, 6.5; F, 8.8. The densities, measured by flotation in mixtures of $CHCl_3/CHBr_3$, are 1.937(8) and 2.072(9) g cm^{-3} for the iron and cobalt compounds, respectively.

2.2. Single-crystal X-ray diffraction

Prismatic single-crystals of compounds (**1**) and (**2**), with dimensions $0.16 \times 0.17 \times 0.20$ and $0.06 \times 0.12 \times 0.30$ mm, respectively, were carefully selected under a polarizing microscope and mounted on a glass fiber. Diffraction data were collected at room temperature on an Enraf-Nonius CAD4 automated diffractometer using graphite-monochromated Mo-$K\alpha$. Details of crystal data and some features of the structure refinement are reported in Table 1. Lattice constants were obtained by a least-squares refinement of the setting angles of 25 reflections in the range $5° < \theta < 15°$. Intensities and angular positions of two standard reflections were measured every hour and showed neither decrease nor misalignment during data collection.

A total of 2081 reflections were measured for (**1**) in the range $1.91° \leqslant \theta \leqslant 0.02°$, of which 1995 were considered to be independent ($R_{int.} = 0.093$), and 1699 were observed after applying the $I > 2\sigma(I)$ criterion. For (**2**) the number of measured reflections was 2080 ($1.91° \leqslant \theta \leqslant 30.00°$), 1984

Table 1
Crystal data and details of the structure refinement procedure for the $(C_6H_{16}N_2)_{0.5}[M(HPO_3)F]$ (M = Fe and Co) phosphites

Formula	$C_6H_{18}F_2Fe_2N_2O_6P_2$	$C_6H_{18}F_2Co_2N_2O_6P_2$
Molecular weight, g mol^{-1}	425.86	432.02
Crystal system	Monoclinic	Monoclinic
Space group	$C2/c$ (no. 15)	$C2/c$ (no. 15)
a, Å	5.607(1)	5.5822(7)
b, Å	21.276(4)	21.325(3)
c, Å	11.652(1)	11.4910(1)
β, deg	93.74(1)	93.464(9)
V, Å^3	1387.1(4)	1365.4(3)
Z	4	4
$\rho_{calc.}$ g cm^{-3}	2.039	2.102
$F(000)$	864	872
T, K	293(2)	293(2)
Radiation, λ(Mo$K\alpha$), Å	0.71073	0.71073
μ (Mo$K\alpha$) mm^{-1}	2.370	2.712
Limiting indices	$-7 < h < 7$, $0 < k < 29$, $0 < l < 16$	$-7 < h < 7$, $0 < k < 30$, $0 < l < 16$
R [$I > 2\sigma(I)$]	$R_1 = 0.059$, w$R_2 = 0.155$	$R_1 = 0.022$, w$R_2 = 0.055$
R [all data]	$R_1 = 0.070$, w$R_2 = 0.165$	$R_1 = 0.029$, w$R_2 = 0.057$
Goodness of fit	1.059	1.038

$R_1 = [\Sigma(|F_o| - |F_c|)]/\Sigma|F_o|$; $wR_2 = [\Sigma[w(|F_o|^2 - |F_c|^2)^2]/\Sigma[w(|F_o|^2)^2]^{1/2}$; $w = 1/[\sigma^2|F_o|^2 + (xp)^2 + (yp)]$; where $p = [|F_o|^2 + 2|F_c|^2]/3$; $x = 0.1287$, $y = 1.0497$ for Fe; $x = 0.032$, $y = 0.4769$ for Co.

being independent reflections ($R_{int.} = 0.014$) and 1717 having $I > 2\sigma(I)$. Data were corrected for Lorentz and polarization effects and for absorption with the empirical ψ scan method [12] using the X-RAYACS program [13]. Direct methods (SHELXS 97) [14] were employed to solve the structure. The metal ions and phosphorus atoms were first located and oxygen, nitrogen and carbon atoms were found from difference Fourier maps. The structures were refined by the full-matrix, least-squares method based on F^2, using the SHELXL 97 computer program [15]. The scattering factors were taken from Ref. [16]. All non-hydrogen atoms were assigned anisotropic thermal parameters. The coordinates of hydrogen atoms of the phosphite anion were obtained from difference Fourier maps. The hydrogen atoms of the *trans*-1,4-diaminocyclohexane cation were geometrically placed in the case of compound (**1**). The high quality of the crystal of compound (**2**) allowed calculation of hydrogen positions from the Fourier maps. Final R factors were $R_1 = 0.070$ (all data) [w$R_2 = 0.165$] for (**1**) and $R_1 = 0.029$ (all data) [w$R_2 = 0.057$] for (**2**). With maximum and minimum peaks in final difference synthesis of 1.780, $-1.653\,e\text{Å}^{-3}$ and 0.614, $-0.358\,e\text{Å}^{-3}$ for (**1**) and (**2**), respectively. The goodness of fit on F^2 was 1.059 for (**1**) and 1.038 for (**2**). Simulations based on the $(C_2H_{16}N_2)_{0.5}[M(HPO_3)F]$ (M = Fe and Co) single-crystal structures was in excellent agreement with the X-ray powder data, indicating the presence of pure polycrystalline phases with high crystallinity. The structure factor parameters have been deposited at the Cambridge Crystallographic Data Centre (CCDC 258110 and 258109, for compounds (**1**) and (**2**), respectively). All drawings were made using ATOMS program [17]. Atomic coordinates are shown in Table 2. Selected bond distances and angles are given in Table 3.

Table 2
Atomic coordinates ($\times 10^4$) and equivalent isotropic displacement parameters ($Å^2 \times 10^3$) for $(C_6H_{16}N_2)_{0.5}[M(HPO_3)F]$ (M = Fe and Co) (e.s.d. in parentheses)

Atom	x	y	z	U_{eq}
$(C_6H_{16}N_2)_{0.5}[Fe(HPO_3)F]$				
Fe(1)	2216(1)	300(1)	3249(1)	14(1)
P(1)	7005(1)	−594(1)	3952(1)	13(1)
F(1)	0	973(1)	2500	17(1)
F(2)	5000	799(1)	2500	18(1)
O(1)	4351(4)	−435(1)	3808(2)	19(1)
O(2)	2294(4)	791(1)	4821(2)	17(1)
O(3)	−1407(4)	−93(1)	3485(2)	21(1)
N(1)	7519(5)	−1189(1)	9481(2)	19(1)
C(1)	6875(6)	−1849(2)	9720(3)	19(1)
C(2)	774(1)	−2037(2)	10925(3)	34(1)
C(3)	7855(9)	−2281(2)	8829(3)	32(1)
$(C_6H_{16}N_2)_{0.5}[Co(HPO_3)F]$				
Co(1)	2195(1)	4702(1)	3233(1)	12(1)
P(1)	6987(1)	5586(1)	3955(1)	11(1)
F(1)	0	4027(1)	2500	14(1)
F(2)	5000	4219(1)	2500	15(1)
O(1)	4325(2)	5429(1)	3803(1)	16(1)
O(2)	2309(2)	4222(1)	4796(1)	15(1)
O(3)	−1407(2)	5088(1)	3467(1)	17(1)
N(1)	2475(3)	6190(1)	5512(1)	16(1)
C(1)	3121(3)	6849(1)	5273(1)	18(1)
C(2)	2200(5)	7040(1)	4056(2)	31(1)
C(3)	2154(4)	7276(1)	6188(2)	29(1)

2.3. Physicochemical characterization techniques

The IR spectra (KBr pellets) were obtained with a Nicolet FT-IR 740 spectrophotometer in the 400–4000 cm^{-1} range. The Raman spectra were recordered in the 200–3000 cm^{-1} range, with a Nicolet 950FT spectrophotometer equipped with a neodymium laser emitting at 1064 nm. Diffuse reflectance spectra were registered at room temperature on a Cary 2415 spectrometer in the 210–2000 nm range. Magnetic measurements, on powdered samples, were performed in the temperature range 2.0–300 K, using a Quantum Design MPMS-7 SQUID magnetometer. The magnetic field was approximately 0.1 T, a value within the range of linear dependence of magnetization vs. magnetic field, even at 2.0 K.

3. Results and discussion

3.1. Thermal behavior

Thermogravimetric analysis was carried out under air in an SDC 2960 Simultaneous DSC-TGA TA Instrument. Crucibles containing ca. 20 mg of sample were heated at 5 °C min^{-1} in the temperature range 30–800 °C. The decomposition curves of the $(C_6H_{16}N_2)_{0.5}[M(HPO_3)F]$ phases reveal a continuous mass loss with superimposed steps between 300 and 700 or 800 °C for (**1**) and (**2**), respectively. These losses correspond to approximately 33.0% or 33.5% for the iron and cobalt compound, respectively, and are in good agreement with the calculated values of 36% or 35.6% for the calcination of the *trans*-1,4-diaminocyclohexane dication and the elimination of the fluoride ion. The final residue obtained from the thermogravimetric analysis at 800 °C was $Fe(PO_4)$ [$P3_121$, $a = b = 5.027(1)$, $c = 11.234(1)$ Å] [18a] for compound (**1**). For compound (**2**), the inorganic residue after total calcination contains $Co_2(P_2O_7)$ [$P2_1/c$, $a = 13.24(1)$, $b = 8.345(1)$, $c = 9.004(1)$ Å, $\beta = 104.6(1)°$] [18b] and $Co_3(PO_4)_2$ [$P2_1/n$, $a = 7.556(1)$, $b = 8.371(1)$, $c = 5.064(1)$ Å, $\beta = 94.0.0(1)°$] [18c].

The thermal behavior of the $(C_6H_{16}N_2)_{0.5}[M(HPO_3)F]$ (M = Fe and Co) compounds was also studied by time-resolved X-ray thermodiffractometry in an air atmosphere. A PHILIPS X'PERT automatic diffractometer (Cu$K\alpha$ radiation) equipped with a variable-temperature stage (Paar Physica TCU2000) with a Pt sample holder was used in the experiment. The powder patterns were recorded in 2θ steps of 0.02° in the range $5 \leqslant 2\theta \leqslant 45°$, counting for 1 s per step and increasing the temperature at 5 °C min^{-1} from room temperature up to 800 °C. Compound (**1**) is stable up to 320 °C and the intensity of the monitored (020)

Table 3
Selected bond distances (Å) and angles (deg) for $(C_6H_{16}N_2)_{0.5}[M(HPO_3)F]$ (M = Fe and Co) (e.s.d. in parentheses)

Bond distances (Å)			
[FeO_4F_2] octahedron		*[CoO_4F_2] octahedron*	
Fe–O(1)	2.050(2)	Co–F(1)	2.0382(9)
Fe–F(1)	2.053(2)	Co–O(1)	2.039(1)
Fe–O(2)	2.107(2)	Co–O(2)	2.065(1)
Fe–F(2)	2.122(1)	Co–F(2)	2.0925(7)
Fe–O(3)^{i}	2.205(2)	Co–O(3)^{i}	2.140(1)
Fe–O(3)	2.230(2)	Co–O(3)	2.204(1)
[HPO_3] tetrahedron		*[HPO_3] tetrahedron*	
P–O(3)^{ii}	1.513(2)	P–O(3)^{ii}	1.519(1)
P–O(2)^{iii}	1.516(2)	P–O(2)^{iii}	1.520(1)
P–O(1)	1.524(2)	P–O(1)	1.523(1)
P–H(1)	1.32(1)	P–H(1)	1.34(2)
$(H_3N(CH_2)_6NH_3)^{2+}$			
N(1)–C(1)	1.482(4)	N(1)–C(1)	1.481(2)
C(1)–C(2)	1.510(5)	C(1)–C(2)	1.515(2)
C(1)–C(3)	1.515(5)	C(1)–C(3)	1.515(2)
C(2)–C(3)^{iv}	1.520(6)	C(2)–C(3)^{v}	1.532(3)
C(3)–C(2)^{iv}	1.520(6)	C(3)–C(2)^{v}	1.532(3)
Intermetallic M–M			
Fe(1)–Fe(1)^{i}	2.942(1)	Co(1)–Co(1)^{i}	2.8881(5)
Bond angles (deg)			
[FeO_4F_2] octahedron		*[CoO_4F_2] octahedron*	
O(1)–Fe–F(1)	172.76(9)	F(1)–Co–O(1)	173.82(4)
O(1)–Fe–O(2)	97.1(1)	F(1)–Co–O(2)	89.80(4)
F(1)–Fe–O(2)	90.07(8)	O(1)–Co–O(2)	96.34(5)
O(1)–Fe–F(2)	94.71(9)	F(1)–Co–F(2)	86.14(3)
F(1)–Fe–F(2)	85.25(6)	O(1)–Co–F(2)	93.85(4)
O(2)–Fe–F(2)	97.76(8)	O(2)–Co–F(2)	97.03(4)
O(1)–Fe–O(3)^{i}	94.8(1)	F(1)–Co–O(3)^{i}	79.01(4)
F(1)–Fe–O(3)^{i}	78.01(8)	O(1)–Co–O(3)^{i}	94.82(5)
O(2)–Fe–O(3)^{i}	167.30(9)	O(2)–Co–O(3)^{i}	168.03(4)
F(2)–Fe–O(3)^{i}	85.74(1)	F(2)–Co–O(3)^{i}	86.53(4)
O(1)–Fe–O(3)	101.1(1)	F(1)–Co–O(3)	77.53(4)
F(1)–Fe–O(3)	77.45(8)	O(1)–Co–O(3)	101.26(5)
O(2)–Fe–O(3)	92.7(1)	O(2)–Co–O(3)	93.39(5)
F(2)–Fe–O(3)	159.80(7)	F(2)–Co–O(3)	160.58(3)
O(3)^{i}–Fe–O(3)	80.6(1)	O(3)^{i}–Co–O(3)	80.16(5)
[HPO_3] tetrahedron		*[HPO_3] tetrahedron*	
O(3)^{ii}–P–O(2)^{iii}	114.3(1)	O(3)^{ii}–P–O(2)^{iii}	114.35(6)
O(3)^{ii}–P–O(1)	113.4(1)	O(3)^{ii}–P–O(1)	113.43(7)
O(2)^{iii}–P–O(1)	110.9(1)	O(2)^{iii}–P–O(1)	111.24(7)
O(3)^{ii}–P–H(1)	106(2)	O(3)^{ii}–P–H(1)	105(1)
O(2)^{iii}–P–H(1)	106(2)	O(2)^{iii}–P–H(1)	105(1)
O(1)–P–H(1)	106(2)	O(1)–P–H(1)	107(1)
$(H_3N(CH_2)_6NH_3)^{2+}$			
N(1)–C(1)–C(2)	111.0(3)	N(1)–C(1)–C(2)	110.6(1)
N(1)–C(1)–C(3)	110.0(3)	N(1)–C(1)–C(3)	109.9(1)
C(2)–C(1)–C(3)	111.6(3)	C(3)–C(1)–C(2)	111.4(1)
C(1)–C(2)–C(3)^{iv}	111.5(3)	C(1)–C(2)–C(3)^{v}	110.7(1)
C(1)–C(3)–C(2)^{iv}	110.8(3)	C(1)–C(3)–C(2)^{v}	110.3(1)

Symmetry codes: (*i*) $= -x, y, -z+1/2$; (ii) $= x+1, y, z$; (iii) $= -x+1, -y, -z+1$; (iv) $= -x+3/2, -y-1/2, -z+2$; (v) $= -x+1/2, -y+3/2, -z+1$.

diffraction maximum at $2\theta = 8.3^\circ$ remains practically unchanged (Fig. 1a). Above that temperature, a rapid decrease in the crystallinity of the compound takes place, becoming finally amorphous. Thus, in the 320–600 °C range no peaks were observed in the X-ray patterns. These results indicate the collapse of the crystal structure of this compound with the loss of the *trans*-1,4-diaminocyclohexane cation. The maxima observed in the thermodiffractograms recordered in the 600–680 °C range show orthorhombic $Fe(PO_4)$ to be the majority phase [*Cmcm*, $a = 5.227(1)$, $b = 7.770(1)$, $c = 6.322(1)$ Å] [18d] and trigonal $Fe(PO_4)$ the minority phase [$P3_121$, $a = b = 5.027(1)$, $c = 11.234(1)$ Å] [18a]. Above this temperature, in the 680–800 °C range, both the orthorhombic and trigonal $Fe(PO_4)$ phases continue to be present with increasing proportions of trigonal $Fe(PO_4)$. Compound (**2**) is stable up to 320 °C, maintaining a constant intensity of the monitored (020) peak at $2\theta = 8.3^\circ$ (Fig. 1b). Between 280 and 380 °C the existence of an unknown inorganic–organic hybrid cobalt phopshite is observed. This new phase presents low crystallinity making it impossible to study by X-ray diffraction. However, the characterization by IR spectroscopy shows unambiguously the existence of the protonated *trans*-1,4-diaminocyclohexane at approximately 3000 and 1625 cm^{-1}, together with bands belonging to the phosphite group in the 1200–500 cm^{-1} range. Above 380 °C no maximum was observed in the thermodiffractograms, indicating that an amorphous residue is obtained after calcination of the organic molecule. Finally, in the 640–800 °C both $Co_2(P_2O_7)$ [$P2_1/c$, $a = 13.24(1)$, $b = 8.345(1)$, $c = 9.004(1)$ Å, $\beta = 104.6(1)^\circ$] [18b] and $Co_3(PO_4)_2$ [$P2_1/n$, $a = 7.556(1)$, $b = 8.371(1)$, $c = 5.064(1)$ Å, $\beta = 94.00(1)^\circ$] [18c] form the inorganic residue, in good agreement with mass losses observed by thermogravimetry.

3.2. Crystal structures

The isostructural $(C_6N_2H_{16})_{0.5}[M(HPO_3)F]$, $M(II) = Fe$ and Co, compounds exhibit a layered structure with the anionic sheets of formula $[M(HPO_3)F]^-$ extended along the (010) plane. The organic dications are located in the interlayer space and establish both ionic interactions and hydrogen bonds with the inorganic layers (Fig. 2).

In the structure exists only one crystallographically independent metallic cation which is bonded to four oxygen atoms, O(1), O(2), O(3), O(3)^{i} from the phosphite oxoanions and two fluoride anions, F(1) and F(2), giving rise to *cis*-$[MO_4F_2]$ octahedra. Each octahedron shares a face formed by two O(3) oxygen atoms and one F(1) fluoride ion to give dimeric entities of $[M_2O_6F_3]$ formula (Fig. 3). The dimeric entities form chains in which dimer units are linked through two F(2) atoms. In these chains the bond between the octahedra is either via face- or vertex-sharing (Fig. 4). If the link in the chains is face-sharing the distance between the metallic cations is 2.942(1) and 2.8881(5) Å for the iron and cobalt compounds, respectively. When the link in the chains is through a shared vertex, the distance between the metallic centres is

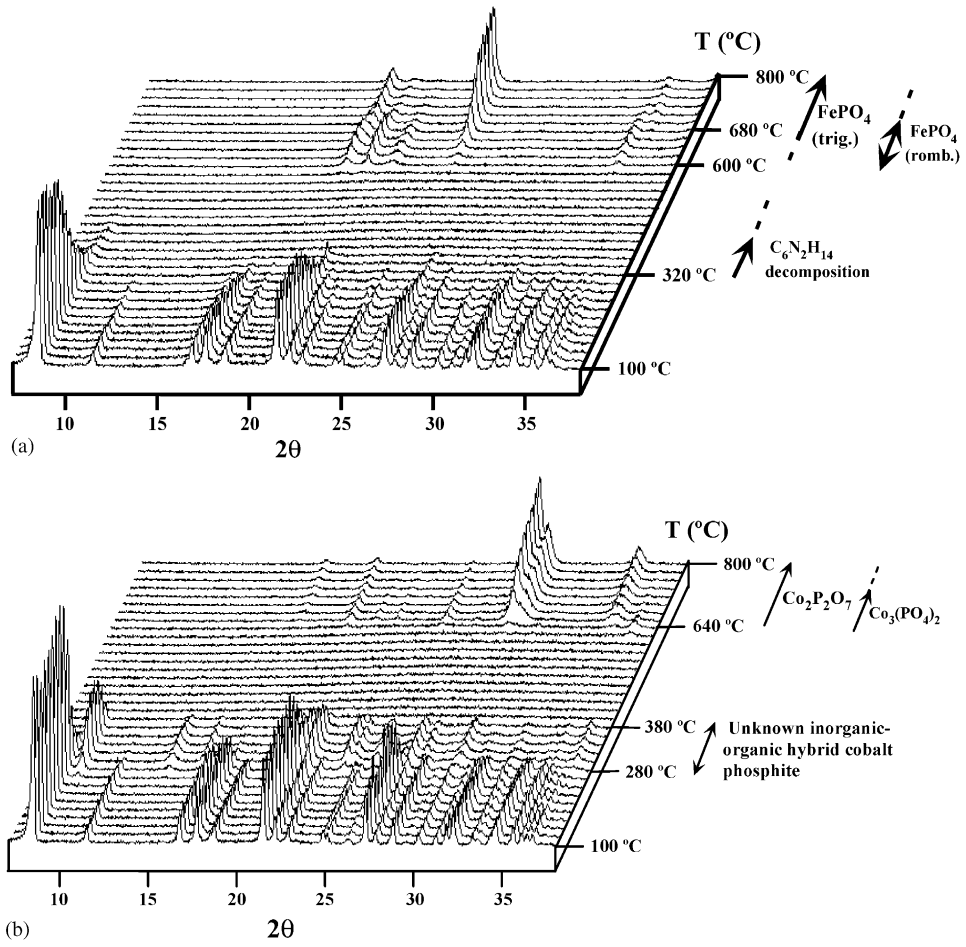

Fig. 1. Thermodiffractograms of (a) $(C_6H_{16}N_2)_{0.5}[Fe(HPO_3)F]$ and (b) $(C_6H_{16}N_2)_{0.5}[Co(HPO_3)F]$. In both cases, the decomposition process and resulting phases are indicated.

longer, 3.675(1) for the iron phase and 3.644(5) Å for the cobalt compound.

In the iron(II) and cobalt(II) compounds the metallic cations of the $[MO_4F_2]$ octahedra are bonded to the oxygen atoms of the phosphite anions with a mean distance of 2.15(8) and 2.11(7) Å, respectively. The mean distance between the metallic centres and the fluoride ions is 2.09(4) Å in compound (**1**) and 2.06(3) Å in compound (**2**). The *cis*–O, F–*M*–O, F angles within the $[MO_4F_2]$ octahedra range from 77.45(8)° to 97.76(8)° for (**1**) and from 77.53(4)° to 101.26(5)° for (**2**). The *trans*-O, F–*M*–O, F angles are in the ranges 159.80(7)–172.76(9)° and 160.58(3)–173.82(4)° for compounds (**1**) and (**2**), respectively.

The P–O bonds of the HPO_3 tetrahedra for (**1**) exhibit a mean value of 1.518(5) Å. In the case of phase (**2**) this mean value is 1.521(2) Å. The O–P–O and H–P–O angles show values typical for the tetrahedral coordination of the phosphite oxoanion.

The *trans*-1,4-diaminocyclohexane dications adopt the chair conformation and are placed in the (100) plane, with the C–NH_3^+ groups along the *a*-direction of the unit cell, perpendicular to the inorganic layers. The protonated organic molecules establish strong hydrogen bonds with the O(1), O(2) and F(2) atoms of the inorganic skeleton, with distances ranging between 1.89(1) and 1.99(1) Å.

3.3. Infrared, Raman and UV-visible spectroscopies

The Infrared and Raman spectra of the $(C_6N_2H_{16})_{0.5}[M(HPO_3)F]$ (M = Fe and Co) phases exhibit in all cases the bands corresponding to the vibrations of the *trans*-1,4-diaminocyclohexane dications and the $(HPO_3)^{2-}$ phosphite anions. Selected bands obtained from both the IR and Raman spectra are given in Table 4. Attempts to obtain the Raman spectrum of the iron(II) phase were unsuccessful due to the calcination of this compound under the laser's Raman radiation. It is worth mentioning the presence of the vibrational modes of the protonated organic molecule, in agreement with the structural data which indicate non-coordination of this cation with the metallic cations. These results are similar to those found for other related phases [19].

The diffuse reflectance spectrum of compound (**1**) shows two bands at approximately 6100 and 9100 cm^{-1}, characteristic of the existence of high spin Fe(II) cation in a slightly distorted octahedral environment. These bands

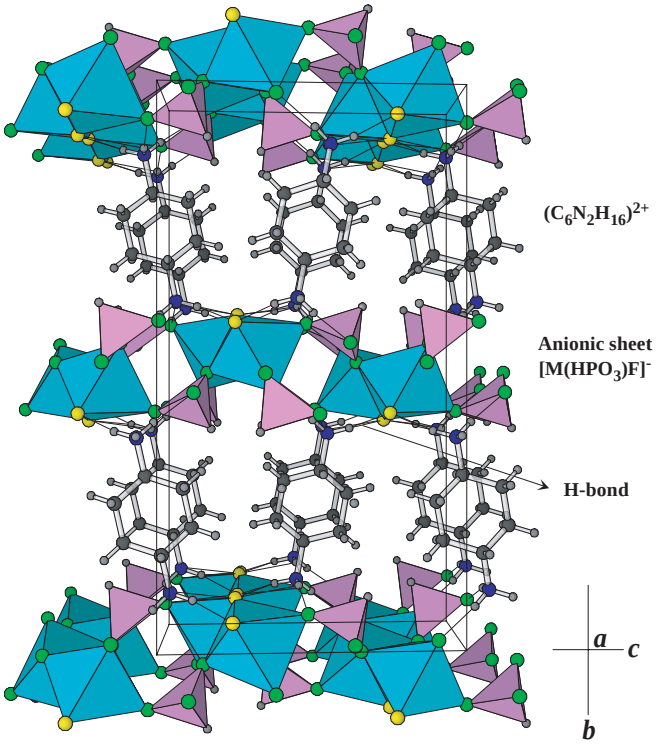

Fig. 2. Polyhedral view of the layered crystal structure for the isostructural $(C_6H_{16}N_2)_{0.5}[M(HPO_3)F]$ (M = Fe and Co) compounds.

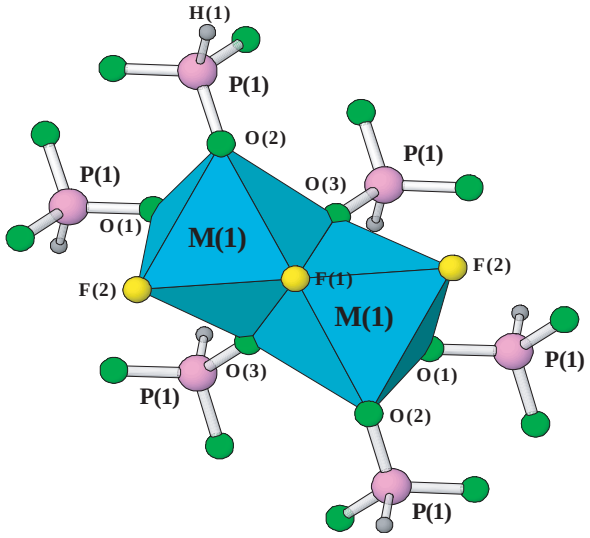

Fig. 3. Polyhedral view of the $[M_2O_6F_3]$ dimeric units for the $(C_6H_{16}N_2)_{0.5}[M(HPO_3)F]$ (M = Fe and Co) compounds.

correspond to the electronic transition from the $^5T_{2g}(^5D)$ fundamental state to the excited $^5E_g(^5D)$, [20,21] which is split as a consequence of the distortion of the $[FeO_4F_2]$ octahedron with Fe–O(3), $O(3)^i$ bond distances of 2.205(2) and 2.230(2) Å being longer than the other Fe–O,F bond lengths in this octahedron, and the $O(3)^i$–Fe–O(3) and F(1)–Fe–$O(3)^i$ bond angles deviating from the ideal value of 90°. The energy associated with this transition corresponds, according to the Tanabe–Sugano diagram, to the Dq parameter. The value obtained is Dq = 790 cm^{-1}, in good agreement with the values observed in related compounds [22]. In the $(C_2H_{10}N_2)[Fe_3(HPO_3)_4]$ [23] organically templated iron(II) phosphite, the absorption spectrum, measured by diffuse reflectance, shows two bands at approximately 6860 and 9265 cm^{-1} for the d^6 high spin cation. Similarly to the iron(II) title compound, these bands correspond to the transition from the ground state $^5T_{2g}(^5D)$ to the excited $^5E_g(^5D)$ which is again split due to steric effects of the irregular $[FeO_6]$ octahedra. The bond distances range from 2.168(3) to 2.171(3) Å and from 2.066(3) to 2.243(3) Å for the $[Fe(1)O_6]$ and $Fe(2)O_6]$ octahedra, respectively, the minimum and maximum *cis*-bond angles being 82.4(1)°, 97.6(1)° and 79.5(1)°, 97.6(1)° for the $Fe^{II}(1)$ and $Fe^{II}(2)$ cations, respectively. The Dq parameter is 805 cm^{-1}, near to that obtained for compound (**1**) reported in this work.

In the case of phase (**2**), the diffuse reflectance spectrum shows bands at approximately 6900, 13,500 and 18,500 cm^{-1}. These bands have been assigned to the allowed transitions from the $^4T_{1g}(^4F)$ fundamental state to the excited levels $^4T_{2g}(^4F)$, $^4A_{2g}(^4F)$ and $^4T_{1g}(^4P)$ for the Co(II) d^7-cation in a slightly distorted octahedral environment [20,21]. The shoulders observed at approximately 7500, 16,500 and 20,490 cm^{-1} have been assigned to the forbidden transitions between the $^4T_{1g}(^4F)$ state and the excited $^2E_{1g}(^2G)$, $^2T_{2g}$, $^2T_{1g}(^2G)$ and $^2A_{1g}(^2G)$ levels. The calculated values of the Dq, B and C parameters are 725, 930 and 4100 cm^{-1}, respectively. The calculated C/B ratio is approximately 4.4. These results are in the range habitually found for octahedrally coordinated Co(II) cations [22]. The reduction of the B-parameter value with respect to that of the free ion (1115 cm^{-1}) suggests a significant covalence in the Co–O/F bonds. $(C_2H_{10}N_2)[Co_3(HPO_3)_4]$ [11d] has an absorption spectrum in which the spin allowed bands corresponding to the electronic transitions $^4T_{1g}(^4F) \rightarrow {}^4T_{2g}(^4F)$, $^4A_{2g}(^4F)$ and $^4T_{1g}(^4P)$ at, approximately, 6450, 13,700 and 18,250 cm^{-1} can be observed, near to those obtained for the compound (**2**) of this work. The Dq parameter has a value of 725 cm^{-1}, whereas the B and C-Racah parameters are 880 and 3950 cm^{-1}, respectively.

3.4. Magnetic properties

The magnetic measurements of $(C_6N_2H_{16})_{0.5}[M(HPO_3)F]$, M(II) = Fe and Co, were carried out on powdered samples from 2.0 K to room temperature. Plots of χ_m and $\chi_m T$ for phase (**1**) are shown in Fig. 5. The molar magnetic susceptibility, χ_m, increases with decreasing temperature and reaches a maximum at approximately 20 K after which the susceptibility decreases to 0.051 $cm^3\,mol^{-1}$ at 2.0 K. This result indicates the existence of an antiferromagnetic ordering at low temperatures. The real symmetry of the crystal field, which is distorted from an ideal octahedral geometry due to steric effects, allows a sufficient splitting of the $^5T_{2g}(^5D)$ ground state of the iron(II) to consider that the

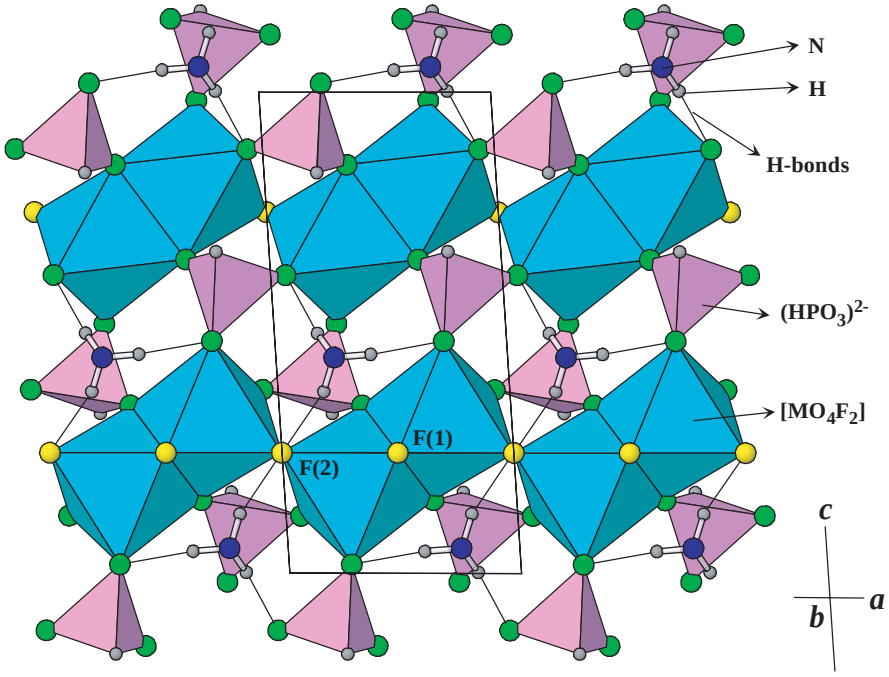

Fig. 4. Polyhedral view of the chains for the $(C_6H_{16}N_2)_{0.5}$ $[M(HPO_3)F]$ (M = Fe and Co) compounds in the (010) plane.

Table 4
Selected bands (values in cm^{-1}) of the $(C_2H_{16}N_2)_{0.5}[M(HPO_3)F]$ [M(II) = Fe and Co] compounds obtained from the IR spectrum for the iron phase, and from the IR and Raman spectra for the cobalt compound

Assignment	M = Fe	M = Co	
	IR	IR	Raman
$\nu(-NH_3)^+$	2945 (s)	2945 (s)	2945 (s)
$\nu(-CH_2-)$	2925 (s)	2925 (s)	2855 (s)
ν(HP)	2340 (m)	2345 (m)	2345 (s)
$\delta(-NH_3)^+$	1630, 1560 (m,s)	1630, 1565 (m,s)	1610 (w)
$\delta(-CH_2-)$	1450–1395 (w)	1450–1395 (w)	1445–1260 (m)
$\nu_{as}(PO_3)$	1110, 1090 (s)	1105 (s)	1090 (w)
$\nu_s(PO_3)$	1055–1025 (m)	1060–1025 (m)	1065–1025 (s)
δ(HP)	1000 (w)	1000 (w)	1005 (s)
$\delta_s(PO_3)$	565, 550 (s)	570, 555 (s)	580 (w)
$\delta_{as}(PO_3)$	495, 475 (s,m)	500, 480 (m)	490 (m)

ν = stretching, δ = deformation, s = symmetric, as = asymmetric, s = strong, m = medium, w = weak.

spin moment is much larger than the orbital moment. As consequence of these features, it is possible to affirm that the thermal evolution of χ_m follows a Curie–Weiss law at temperatures higher than 120 K, the values of the Curie and Curie–Weiss parameters being $2.693\,cm^3\,K\,mol^{-1}$ and $\theta = -4.6$ K, respectively. The calculated value of the g-tensor from the Curie constant is 2.22, in the range habitually found for iron(II) compounds [24]. The $\chi_m T$ product maintains a constant value of $3.65\,cm^3\,K\,mol^{-1}$ between 300 and 150 K. Below this temperature the values of $\chi_m T$ decreases to $0.15\,cm^3\,K\,mol^{-1}$, in good agreement with the existence of antiferromagnetic interactions.

For compound (**2**) the molar magnetic susceptibility shows a maximum at approximately 6.0 K (Fig. 6). Below this temperature the values of χ_m decreases down 2.0 K. Similarly to that described above for the iron(II) phase, it is possible to affirm that the thermal evolution of the molar magnetic susceptibility of (**2**) follows the Curie–Weiss law at high temperatures ($T > 210$ K), with $C_m = 3.512\,cm^3\,K\,mol^{-1}$ and $\theta = -13.59$ K. The calculated value of the g-tensor is 2.74, in the range habitually found for cobalt(II) compounds [24]. The $\chi_m T$ vs. T curve decreases continuously from $3.35\,cm^3\,K\,mol^{-1}$ at 300 K to $0.35\,cm^3\,mol^{-1}$ at 2.0 K, as a consequence of the existence of both antiferromagnetic interactions and the spin–orbit coupling characteristic of cobalt(II) phases [25]. The small value of the ordering temperature in the cobalt compound, in comparison with that of the iron phase, indicates that the antiferromagnetic interactions in the latter compound are stronger.

The $(C_2H_{10}N_2)[M_3(HPO_3)_4]$ (M^{II} = Fe and Co) phases [11d,23] show a distorted octahedral geometry, approximately 11% calculated using the Muetterties and Guggenberger description [26], such that the crystal fields do not correspond to ideal octahedral symmetries, the spin moment being much larger than the orbital one. In this way these compounds follow the Curie–Weiss law. The values of the Curie and Curie–Weiss constants are $C_m = 10.734\,cm^3\,K\,mol^{-1}$, $\theta = -18.30$ K for the iron(II) compound, and $C_m = 11.580\,cm^3\,K\,mol^{-1}$, $\theta = -44.80$ K for the cobalt(II) phase. The compounds exhibit antiferromagnetic couplings.

Taking into account the structural features of the $(C_6H_{16}N_2)_{0.5}[M(HPO_3)F]$ [M(II) = Fe and Co] title compounds, in which the layered structure is formed by chains

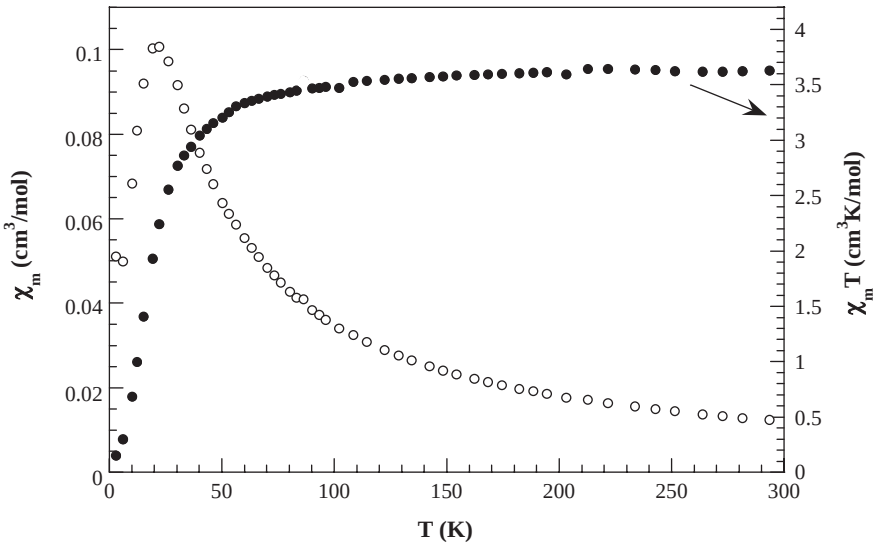

Fig. 5. Thermal evolution of χ_m and $\chi_m T$ for $(C_6H_{16}N_2)_{0.5}[Fe(HPO_3)F]$.

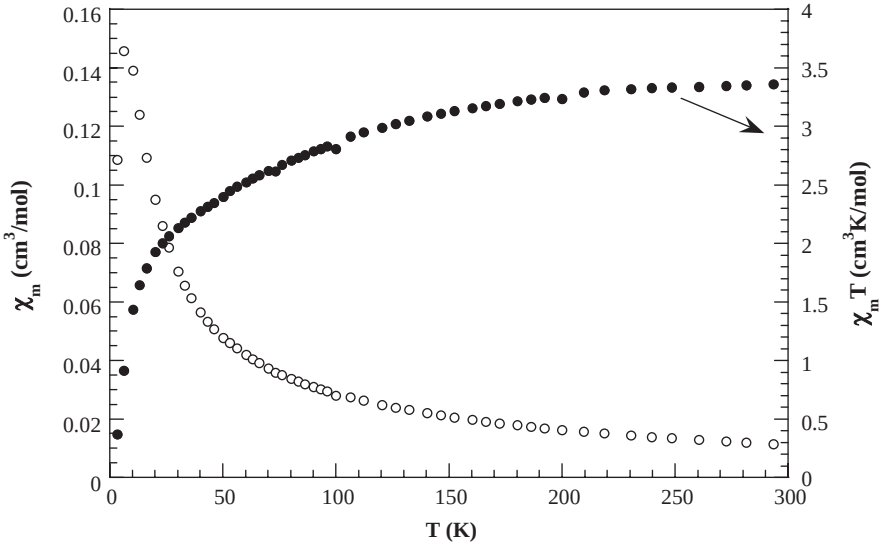

Fig. 6. Thermal evolution of χ_m and $\chi_m T$ for $(C_6H_{16}N_2)_{0.5}[Co(HPO_3)F]$.

of face-sharing dimeric entities (see Figs. 3 and 4), several magnetic exchange pathways can take place: (i) Direct intradimeric interactions involving two t_{2g} orbitals from the Fe(II) cations and one t_{2g} orbital belonging to the Co(II) cations, that ought to lead to antiferromagnetic couplings. (ii) Superexchange intradimeric interactions via O(3) and F(1) atoms involving metal e.g. (dz^2 and $d_x{}^2-y^2$) orbitals from face-sharing MO_6F_3 dimeric units. The values of the angles $M(1)$–F(1)–$M(1)$ and $M(1)$–O(3)–$M(1)$ are approximately 91° and 83°, respectively, so, both ferro or antiferromagnetic interactions could be given [27]. (iii) Superexchange interaction through the F(2) atoms linking the dimeric units along the chains. The value of the angle $M(1)$–F(2)–$M(1)$ of approximately 120° should lead to antiferromagnetic interactions [25]. (iv) Superexchange interactions via $(HPO_3)^{2-}$ anions, linked to the chains in two dimensions, should favor the antiferromagnetic couplings.

4. Concluding remarks

Two new organically templated materials based on the iron(II) and colbalt (II) cations and the phosphite oxoanions have been synthesized using mild solvothermal conditions under autogeneous pressure. The inorganic framework consists of sheets formed from chains of dimeric units. The *trans*-1,4-diaminocyclohexane organic dications are located in the interlayer space, establishing both ionic interactions and hydrogen bonds with the inorganic sheets. The IR and Raman spectra of both compounds show the bands belonging to the $(HPO_3)^{2-}$ phosphite oxoanions and the protonated organic molecule.

The presence of one δ(P–H) band in the IR and Raman spectra are consistent with the existence of one crystallographicaly independent phosphite group in the crystal structure of these phases. The values of the Dq and Racah parameters calculated from the diffuse reflectance spectra are in the range habitually found for these cations in slightly distorted octahedral environment. The magnetic measurements indicate antiferromagnetic couplings which are stronger in the iron(II) phase than in the isostructural cobalt(II) compound.

Acknowledgments

This work has been financially supported by the "Ministerio de Educación y Ciencia" (MAT-2004-02071) the "Universidad del País Vasco" (UPV/EHU) (9/UPV00130.310-15967/2004; 9/UPV00169.310-13494/2001). The authors thank the technicians of SGIker, Dr. J.P. Chapman, financed by the "National Program for the Promotion of Human Resources" within the National Plan of Scientific Research, Development and Innovation—"Ministerio de Ciencia y Tecnología" and "Fondo Social Europeo (FSE)", for the X-ray diffraction. Dr. S. Fernandez wishes to thank the Gobierno Vasco/Eusko Jaurlaritza for funding.

References

[1] A.K. Cheetham, G. Férey, T. Loiseau, Angew. Chem. Int. Ed. 149 (2000) 3268.
[2] C. Cascales, B. Gomez-Lor, E. Gutierrez-Puebla, M. Iglesias, M.A. Monge, C. Ruiz-Valero, N. Snejko, Chem. Mater. 14 (2002) 677.
[3] G.-Y. Yang, S.C. Sevov, J. Am. Chem. Soc. 121 (1999) 8389.
[4] H. Li., M. Eddaoudi, D.A. Richardson, O.M. Yaghi, J. Am. Chem. Soc. 120 (1998) 8567.
[5] G. Férey, Chem. Mater. 13 (2001) 3084.
[6] C.L. Bowes, G.A. Ozin, Adv. Mater. 8 (1996) 13.
[7] O. Conard, C. Jansen, B. Krebs, Angew. Chem. Int. Ed. 37 (1998) 3208.
[8] (a) D.W. Breck, Zeolite Molecular Sieves, Wiley, New York, 1974; (b) W.M. Meier, D.H. Oslen, C. Baerloche, Atlas of Zeolite Structure Types, Elsevier, London, 1996.
[9] M. Mrak, U. Kolitsch, C. Lengauer, V. Kaucic, E. Tillmanns, Inorg. Chem. 42 (2003) 598.
[10] (a) M. Shieh, K.J. Martin, P.J. Squattrito, A. Clearfield, Inorg. Chem. 29 (1990) 958; (b) F. Sapiña, P. Gomez, M.D. Marcos, P. Amoros, R. Ibañez, D. Beltran, Eur. J. Solid State Inorg. Chem. 26 (1989) 603; (c) M.D. Marcos, P. Amoros, A. Beltran, R. Martinez, J.P. Attfield, Chem. Mater. 5 (1993) 121; (d) M.P. Attfield, R.E. Morris, A.K. Cheetham, Acta Crystallogr. C 50 (1994) 981; (e) M.D. Marcos, P. Amoros, A. Le Bail, J. Solid State Chem. 107 (1993) 250.
[11] (a) G. Bonavia, J. DeBord, R.C. Haushalter, D. Rose, J. Zubieta, Chem. Mater. 7 (1995) 1995; (b) S. Fernandez, J.L. Mesa, J.L. Pizarro, L. Lezama, M.I. Arriortua, R. Olazcuaga, T. Rojo, Chem. Mater. 12 (2000) 2092; (c) S. Fernandez, J.L. Pizarro, J.L. Mesa, L. Lezama, M.I. Arriortua, R. Olazcuaga, T. Rojo, Inorg. Chem. 40 (2001) 3476; (d) S. Fernandez, J.L. Pizarro, J.L. Mesa, L. Lezama, M.I. Arriortua, T. Rojo, Int. J. Inorg. Mater. 3 (2001) 331; (e) S. Fernandez, J.L. Mesa, J.L. Pizarro, L. Lezama, M.I. Arriortua, T. Rojo, Chem. Mater. 14 (2002) 2300; (f) S. Fernandez, J.L. Mesa, J.L. Pizarro, L. Lezama, M.I. Arriortua, T. Rojo, Angew. Chem. Int. Ed. 41 (2002) 3683; (g) S. Fernandez, J.L. Mesa, J.L. Pizarro, L. Lezama, M.I. Arriortua, T. Rojo, Chem. Mater. 15 (2003) 1204; (h) S. Fernández, J.L. Mesa, J.L. Pizarro, J.S. Garitaonaindia, M.I. Arriortua, T. Rojo, Angew. Chem. Int. Ed. 43 (2004) 977.
[12] A.C.T. North, D.C. Philips, F.S. Mathews, Acta Crystallogr. A 24 (1968) 351.
[13] A. Chandrasekaran, X-RAYACS: Program for Single Crystal X-ray Data Corrections, Chemistry Department, University of Massachusetts, Amherst, USA, 1998.
[14] G.M. Sheldrick, SHELXS 97: Program for the Solution of Crystal Structures, University of Göttingen, Germany, 1997.
[15] G.M. Sheldrick, SHELXL 97: Program for the Refinement of Crystal Structures, University of Göttingen, Germany, 1997.
[16] International Tables for X-ray Crystallography, vol. IV, Kynoch Press, Birmingham, England, 1974, p. 99.
[17] E. Dowty, ATOMS: a computer program for displaying atomic structures; Shape Software, 521 Hidden Valley Road, Kingsport, TN, 1993.
[18] Powder Diffraction File—Inorganic and Organic, ICDD, Files No. (a) 84–876; (b) 70–1491; (c) 77–0224; (d) 30–659, Pennsylvania, USA, 1995.
[19] (a) A. Gharbi, A. Jouini, M.T. Averbuch-Pouchot, A. Durif, J. Solid State Chem. 111 (1994) 330; (b) D. Dolphin, A.E. Wick, Tabulation of Infrared Spectral Data, Wiley, New York, 1977; (c) M. Tsuboi, J. Am. Chem. Soc. 79 (1957) 1351; (d) K. Nakamoto, Infrared and Raman Spectra of Inorganic and Coordination Compounds, Wiley, New York, 1997.
[20] Y. Tanabe, S.J. Sugano, Phys. Soc. Japan 9 (1954) 753.
[21] L.E. Orgel, J. Chem. Phys. 23 (1955) 1004.
[22] A.B.P. Lever, Inorganic Electronic Spectroscopy, Elsevier Science Publishers B.V., Amsterdam, Netherlands, 1984.
[23] U.-C. Chung, J.L. Mesa, J.L. Pizarro, L. Lezama, J.S. Garitaonaindia, J.P. Chapman, M.I. Arriortua, J. Solid State Chem. 177 (2004) 2705.
[24] R.L. Carlin, Magnetochemistry, Springer, Berlin, Heidelberg, 1986.
[25] J.M. Dunn, Trans. Faraday Soc. 57 (1961) 1441.
[26] E.L. Muetterties, L.J. Guggenberger, J. Am. Chem. Soc. 96 (1974) 1748.
[27] J.B. Goodenough, Magnetism and the Chemical Bond, Interscience, New York, 1963.